

ARID5B influences B-cell development and function in mouse

Charnise Goodings,^{1*} Xujie Zhao,^{1*} Shannon McKinney-Freeman,² Hui Zhang³ and Jun J. Yang^{1,4}

¹Department of Pharmaceutical Sciences, St. Jude Children's Research Hospital, Memphis, TN, USA; ²Department of Hematology, St. Jude Children's Research Hospital, Memphis, TN, USA; ³Department of Hematology/Oncology, Shanghai Children's Medical Center, Shanghai, China and ⁴Department of Oncology, St. Jude Children's Research Hospital, Memphis, TN, USA.

**CG and XZ contributed equally as co-first authors.*

Correspondence: J. J. Yang

jun.yang@stjude.org

Received: March 29, 2022.

Accepted: July 29, 2022.

Prepublished: August 4, 2022.

<https://doi.org/10.3324/haematol.2022.281157>

©2023 Ferrata Storti Foundation

Published under a CC BY-NC license



Histology

Following euthanasia, tissues were collected and fixed in 10% neutral buffered formalin, embedded in paraffin, and 4- μ m sections were used for IHC analysis. All assay steps for CD3 (Santa Cruz #sc-1127, 1:1000, TX, USA), including deparaffinization, rehydration, and epitope retrieval (using CC1, Ventana Medical Systems, AZ, USA), were performed on the Ventana Discovery Ultra autostainer. All assay steps for B220/CD45R (PharMingen #553084, 1:8000, CA, USA) were performed on the Leica BOND-MAX automated stainer, using epitope retrieval solution ER2 (Leica Biosystems Inc., IL, USA). Tissue sections were examined by a board-certified veterinary pathologist (J.L.) who was blinded to the study design.

Mitochondria respiration analysis

The Seahorse analyzer XF24 (Agilent, CA, USA) was used to continuously monitor OCR as previously described(32). Briefly, cells were attached to CellTak-coated plates and then incubated with XF Base medium. Basal OCR were assessed, followed by oligomycin (final concentration 1 μ M), FCCP (1 μ M), and rotenone/antimycin A (0.5 μ M each).

Statistical analyses

All the plots and statistical analyses were performed using Graphpad Prism (version 9). The student's *t*-test (2-sided) was used to calculate the *P*-value for all analyses unless otherwise indicated. All experiments were generally repeated with at least three mice. In all figures, a single data point represents an individual mouse, and bars indicate the mean \pm SEM.

Supplementary table 1. Primers for genotyping

Gene	Forward	Reverse
Vav1-tTA	TGCCAACAAGGTTTTTCACTAGAGA	CTCTTGATCTTCCAATACGCAACCTA
Arid5b-tetO	ACAAGTTTGGAGAGAATGTTGAGTTCA	TTTTCTCTATCACTGATAGGGAGTGGTAA
Arid5b-wildtype	CAATCCATTCAAGCCAACAAGTTTG	AGCGAAATACCTGGAGTGAGTTG

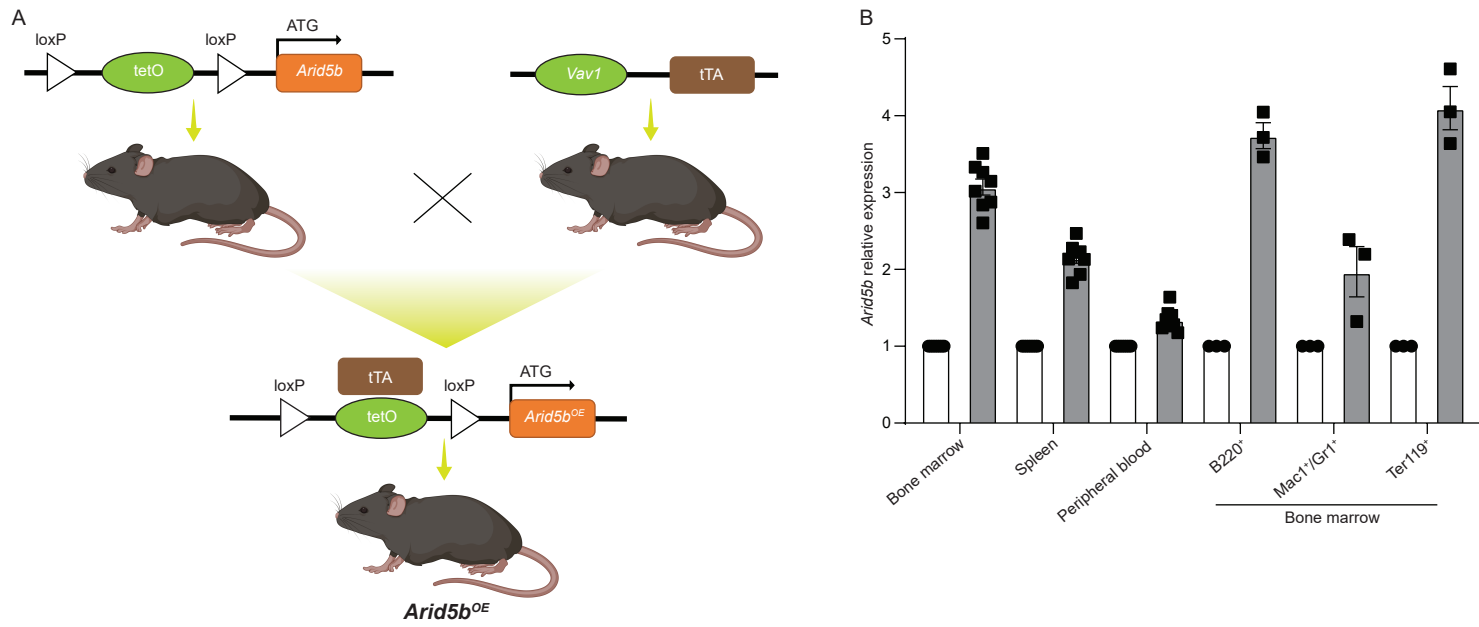
Supplementary table 2. Primers for quantitative real-time PCR

Gene	Forward	Reverse
ACTB	GTTGTCGACGACGAGCG	GCACAGAGCCTCGCCTT
Arid5b	AATCTTGTCCTTGCGACT	CAGAATGCGCCCATTTGACA

Supplementary table 3. Antibodies for flow

Antibodies	Clones	Supplier
CD117 (c-kit)	2B8	BD Biosciences
CD11b (Mac1)	M1/70	BD Biosciences
CD127-APC	SB/199	BD Biosciences
CD135	A2F10.1	BD Biosciences
CD138	281-2	BD Biosciences
CD150	mShad150	eBiosciences
CD179a	R3/VpreB	BD Biosciences
CD179b	LM34	BD Biosciences
CD19	1D3	BD Biosciences
CD21/35	7G6	BD Biosciences
CD23	B3B4	BD Biosciences
CD24	M1/69	BD Biosciences
CD249 (BP-1)	BP-1	BD Biosciences
CD3	145-2C11	BD Biosciences
CD34-Alexa700	RAM34	BD Biosciences
CD38	90/CD38	BD Biosciences
CD4	GK1.5	BD Biosciences
CD43	S7	BD Biosciences
CD45R (B220)	RA3-6B2	BD Biosciences
CD48	HM48-1	BD Biosciences
CD5	53-7.3	BD Biosciences
CD69	H1.2F3	BD Biosciences
CD71	C2	BD Biosciences
CD86	GL1	BD Biosciences
CD8a	53-6.7	BD Biosciences
CD93	AA4.1	BD Biosciences
FcR II/III (CD16/32)	2.4G2	BD Biosciences
GL7	GL7	BD Biosciences
IgD	11-26c.2a	BD Biosciences
IgM	R6-60.2	BD Biosciences
Ly-6A/E (Sca-1)	D7	BD Biosciences
Ly-6G and Ly-6C (Gr1)	RB6-8C5	BD Biosciences
streptavidin		BD Biosciences
TCR-B	H57-597	BD Biosciences
Ter119	TER-119	BD Biosciences

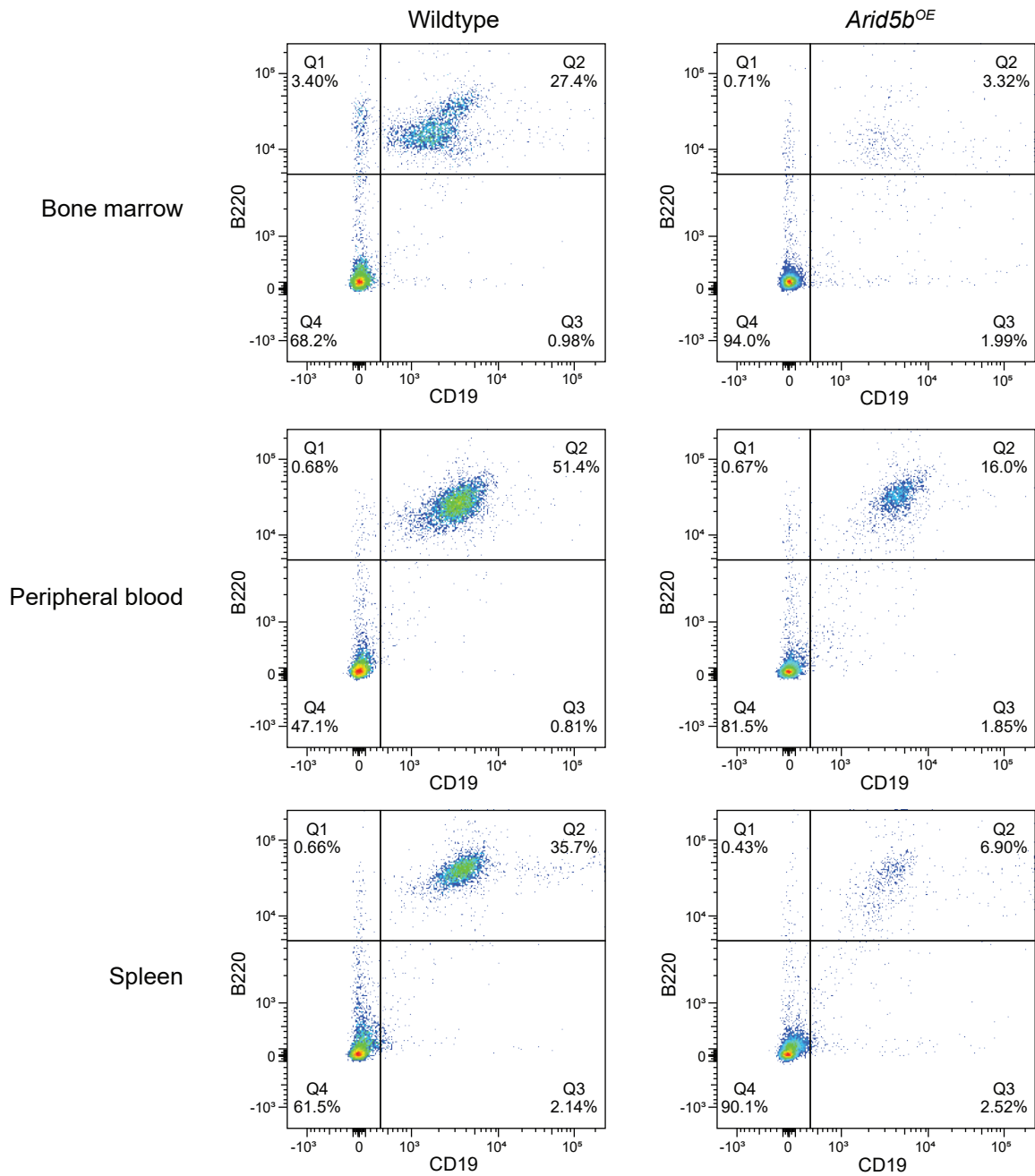
Figure S1



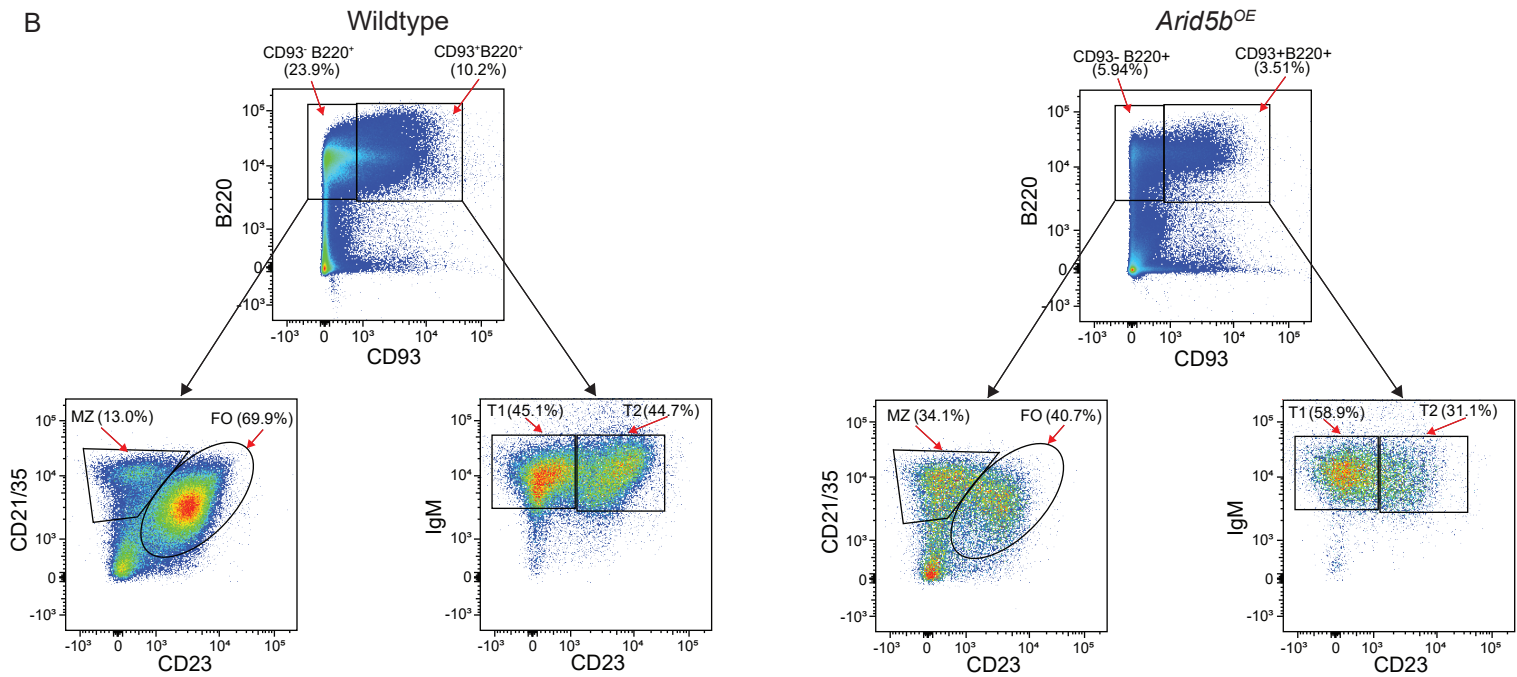
Supplementary Figure 1. Generation of *Arid5b* overexpression mice. (A) Schematic diagram of the *Vav1*-tTA driven overexpression of *Arid5b* mouse model. **(B)** Relative *Arid5b* expression in *Arid5b*^{OE} mice (solid bars) and wildtype littermates (open bars).

Figure S2

A



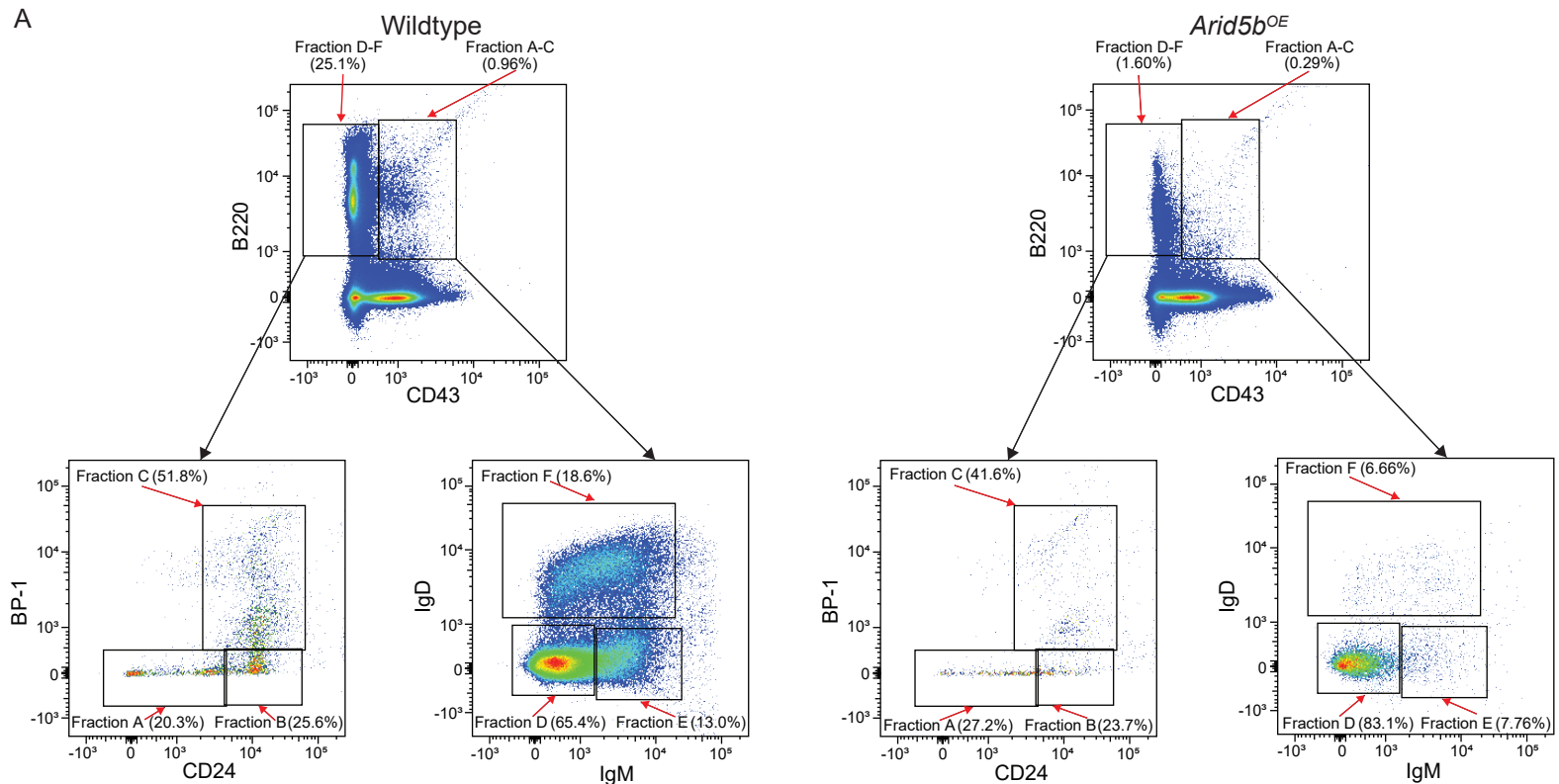
B



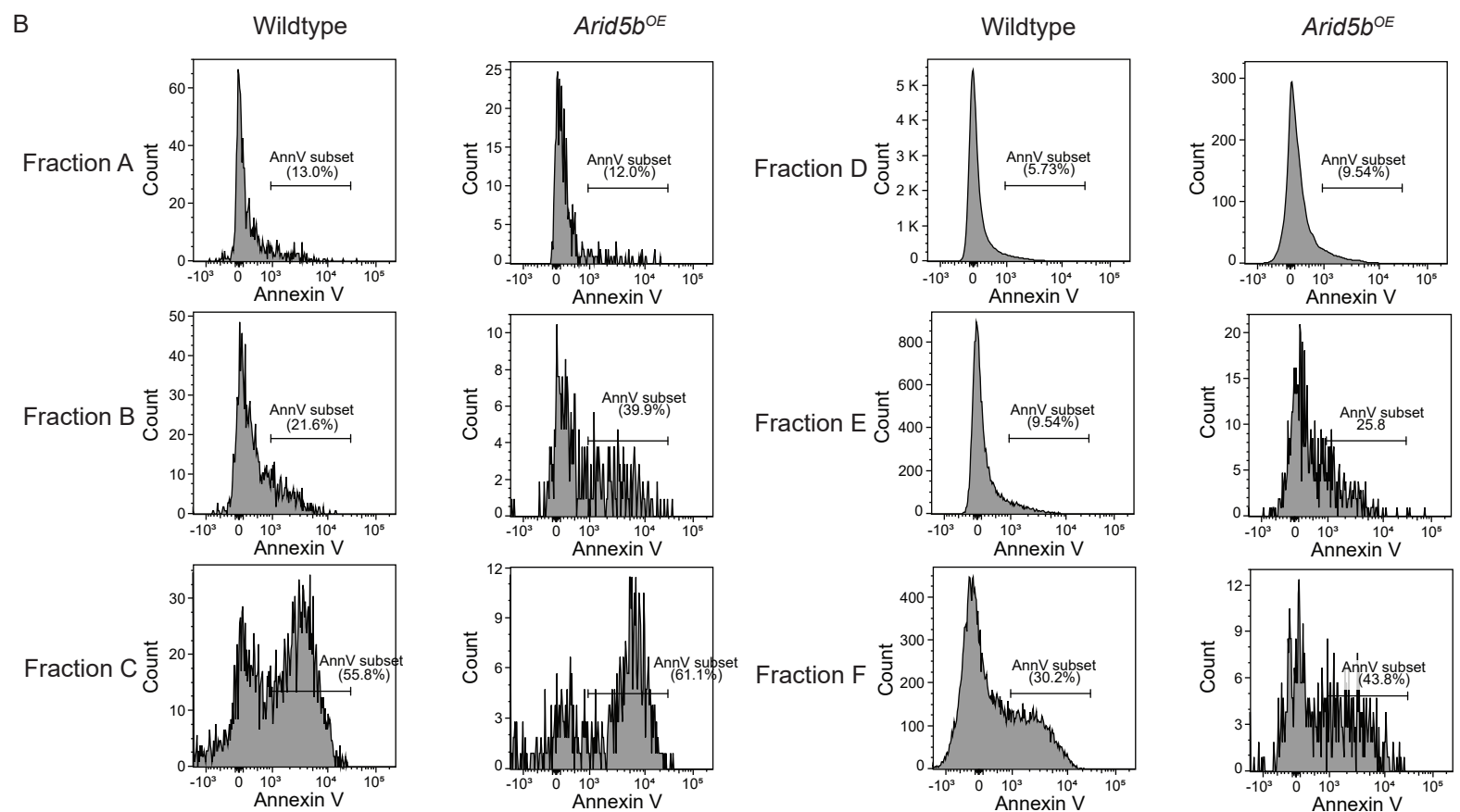
Supplementary Figure 2. Representative flow cytometry plots of B cell subset. (A) Representative flow cytometry plots of B220/CD19 B cell subsets in bone marrow, peripheral blood, and spleen. **(B)** Representative flow cytometry plots of MZ, FO, T1, and T2 B cell subsets in spleen.

Figure S3

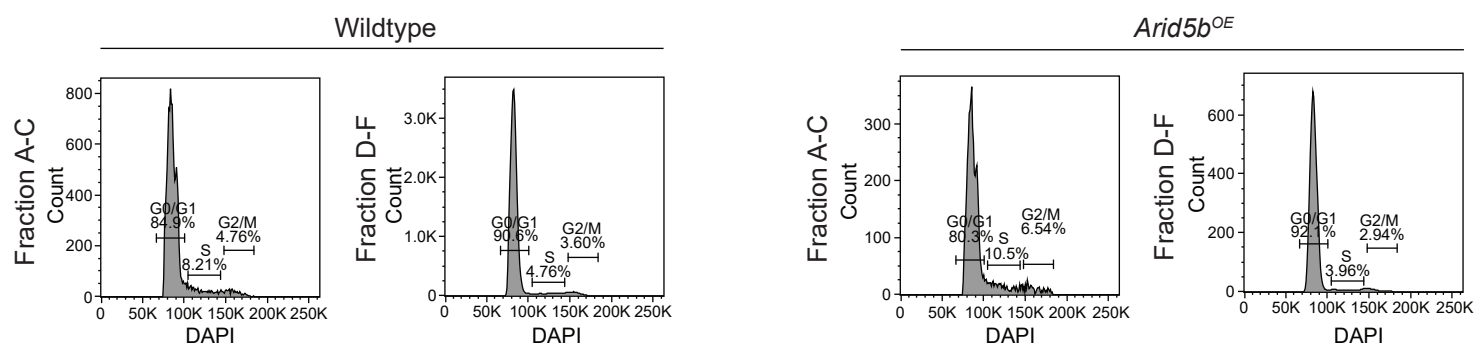
A



B

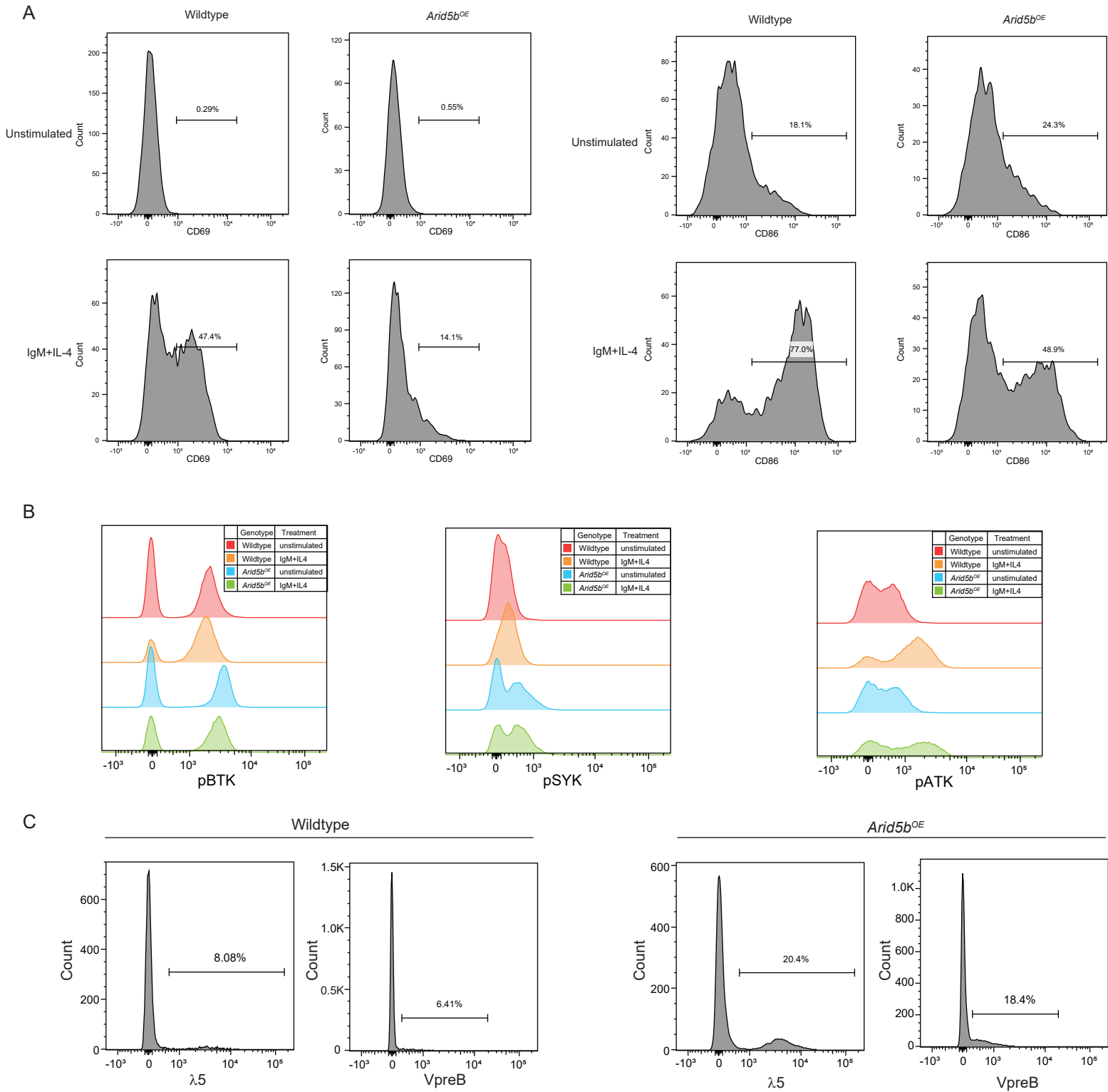


C



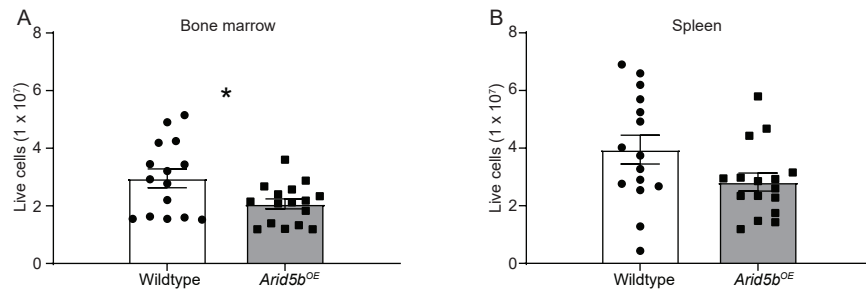
Supplementary Figure 3. Representative flow cytometry plots of Hardy fraction B cells. (A) Representative flow cytometry plots of Hardy fraction B cell subsets in bone marrow. (B) Representative flow cytometry plots of apoptotic Hardy fraction B cells in bone marrow. (C) Representative flow cytometry plots of cell cycle distribution of Hardy fraction B cells in bone marrow.

Figure S4



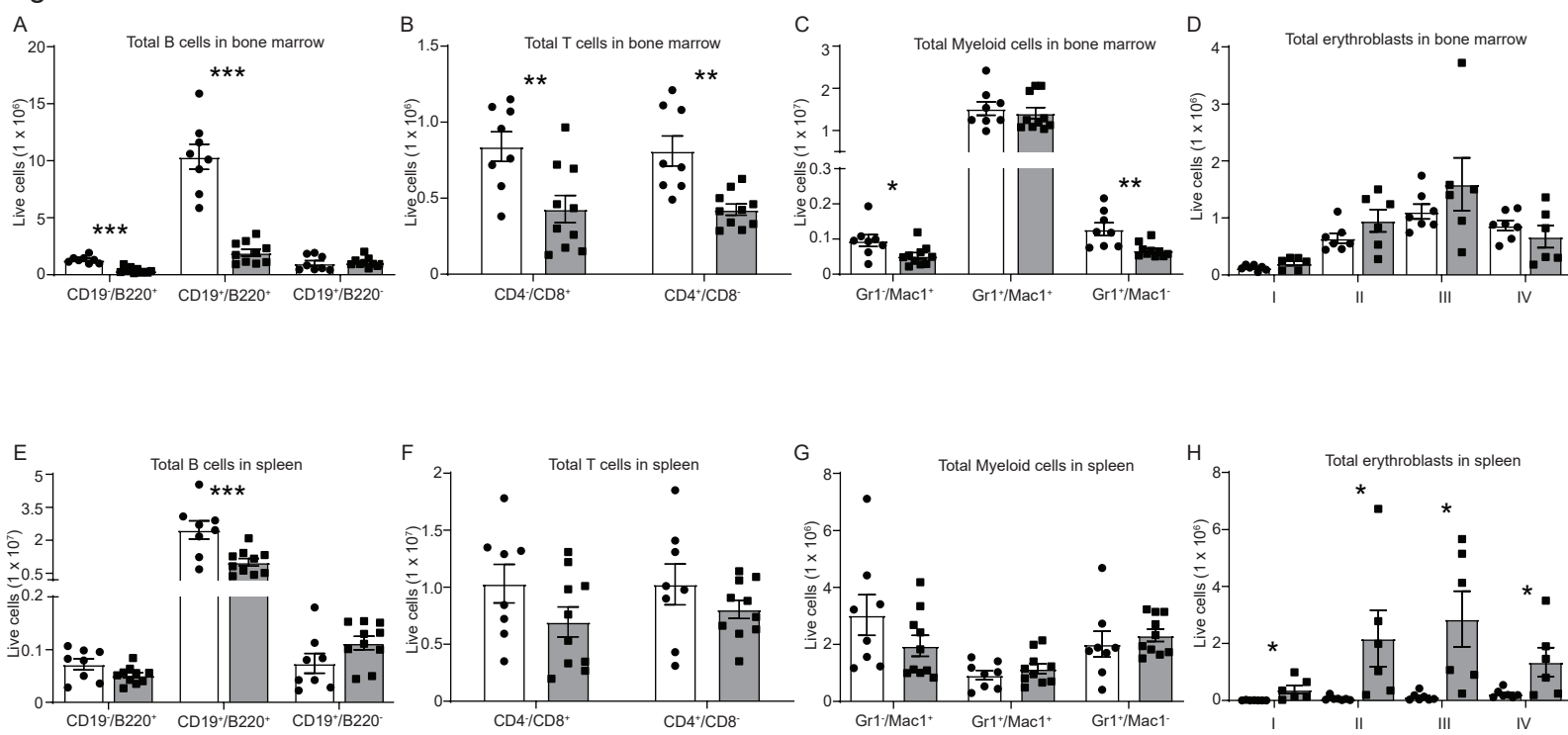
Supplementary Figure 4. Representative flow cytometry plots of surface markers of B cells. (A) Representative flow cytometry plots of B cell activation markers (CD69 and CD86) expression in response to stimulation by IgM+IL-4. **(B)** Representative flow cytometry plots of expressions of pBTK, pSYK, and pATK in B cells. **(C)** Representative flow cytometry plots of expressions of $\lambda 5$ and VpreB on CD19⁺ B cells.

Figure S5



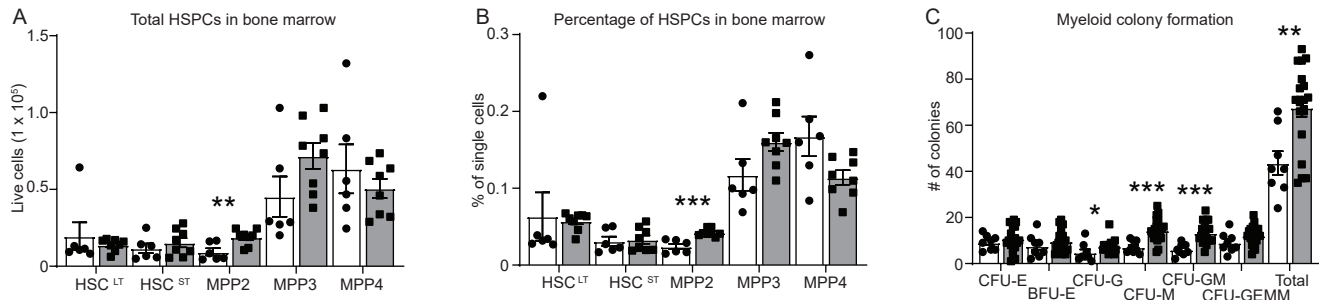
Supplementary Figure 5. Bone marrow and spleen cellularity of *Arid5b*^{OE} mice. (A) Total cellularity in the bone marrow of *Arid5b*^{OE} mice (solid bars, n=16) and wildtype littermates (open bars, n=15). (B) Total cellularity in the spleen of *Arid5b*^{OE} mice (solid bars, n=16) and wildtype littermates (open bars, n=15). *P* value was estimated by two-tail *t* test. *: *P*<0.05.

Figure S6



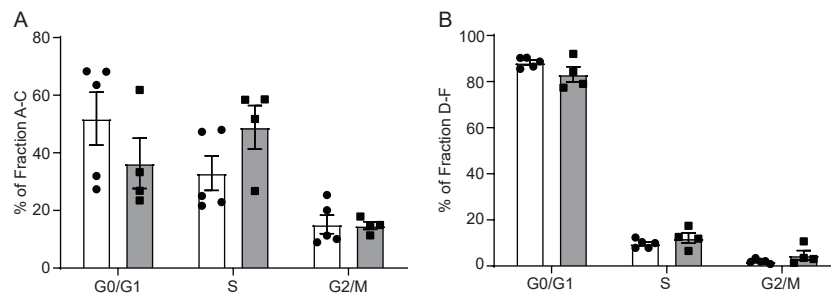
Supplementary Figure 6. Effects of *Arid5b*^{OE} on lymphoid, myeloid, and erythroid lineage maturation in the bone marrow and spleen. (A, E) Total B220⁺ and CD19⁺ B cells in the bone marrow and spleen of *Arid5b*^{OE} mice (solid bars, n=10) compared to wildtype littermates (open bars, n=8). (B, F) Total CD4⁺ and CD8⁺ T cells in the bone marrow and spleen of *Arid5b*^{OE} mice (solid bars, n=10) compared to wildtype littermates (open bars, n=8). (C, G) Total Mac1⁺ and Gr1⁺ myeloid cells in the bone marrow and spleen of *Arid5b*^{OE} mice (solid bars, n=10) compared to wildtype littermates (open bars, n=8). (D, H) Total Ter119⁺ and CD71⁺ erythroblasts in the bone marrow and spleen of *Arid5b*^{OE} mice (solid bars, n=6) compared to wildtype littermates (open bars, n=7). *P* value was estimated by two-tail *t* test. *: *P*<0.05; **: *P*<0.01; ***: *P*<0.001.

Figure S7



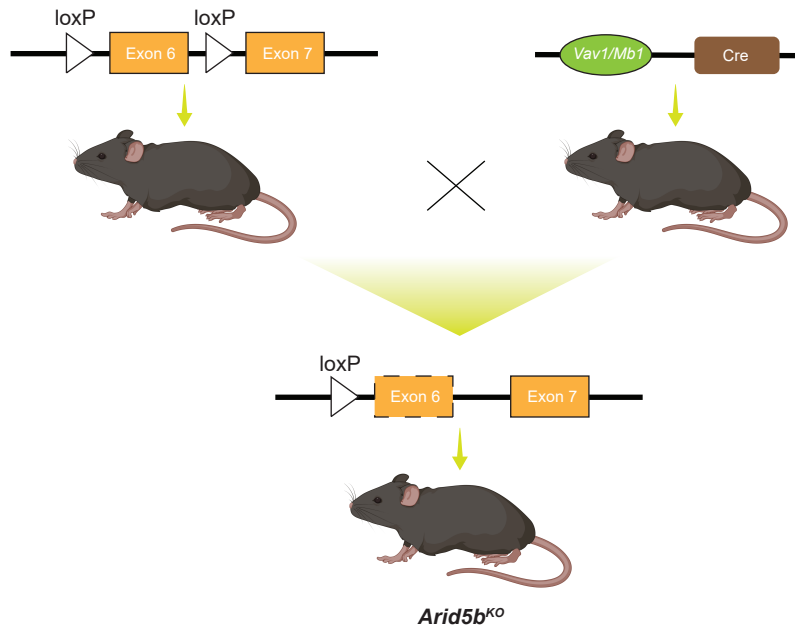
Supplementary Figure 7. Total number and frequency of hematopoietic stem and/or progenitor cells in *Arid5b*^{OE} mice. (A) Total number of hematopoietic stem and progenitor cells in the bone marrow of *Arid5b*^{OE} mice (solid bars, n=8) and wildtype littermates (open bars, n=6). (B) Percentage of hematopoietic stem and progenitor cells in the bone marrow of *Arid5b*^{OE} mice (solid bars, n=8) and wildtype littermates (open bars, n=6). (C) Myeloid colony-forming unite per 20,000 bone marrow cells from *Arid5b*^{OE} (n=20) or wildtype (n=8) mice done in replicate, using MethoCult M3434. P value was estimated by two-tail t test. *: P<0.05; **: P<0.01; ***: P<0.001.

Figure S8



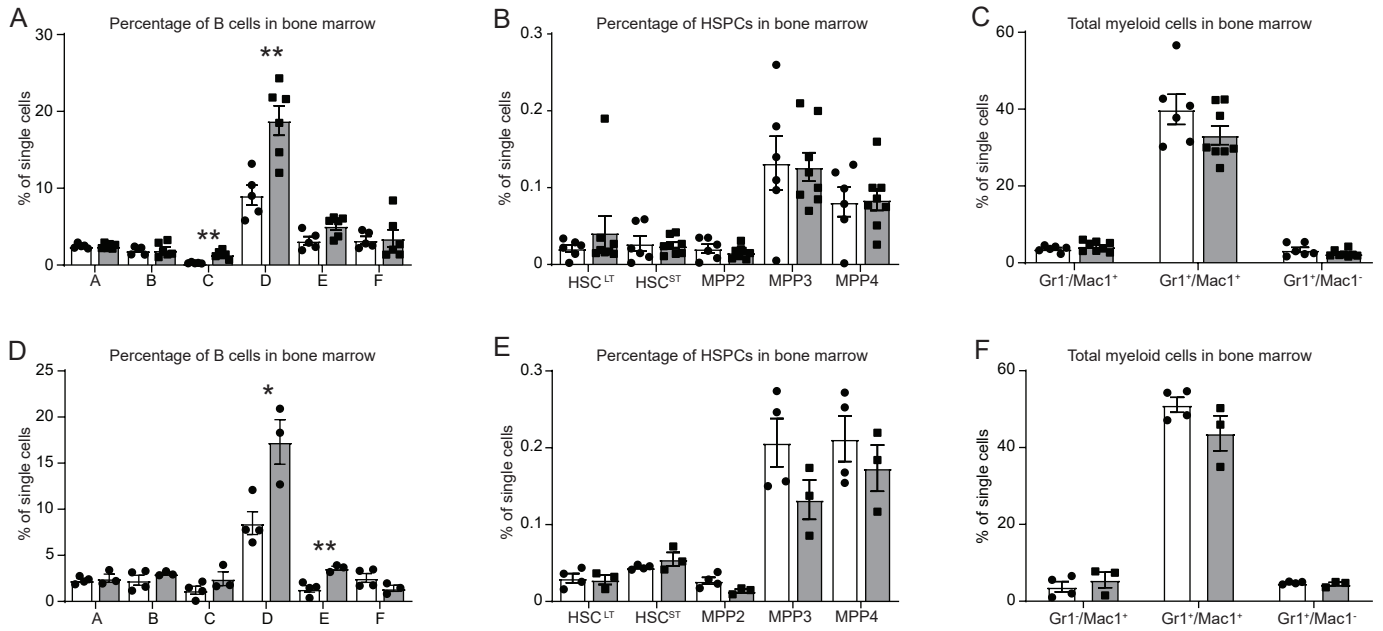
Supplementary Figure 8. Cell cycle distribution of bone marrow B cell subsets from *Arid5b*^{OE} mice. (A) Cell cycle profile of Hardy fraction A-C in the bone marrow of *Arid5b*^{OE} mice (solid bars, n=4) and wildtype littermates (open bars, n=5). (B) Cell cycle profile of Hardy fraction D-F in the bone marrow of *Arid5b*^{OE} mice (solid bars, n=4) and wildtype littermates (open bars, n=5). *P* value was estimated by two-tail *t* test.

Figure S9



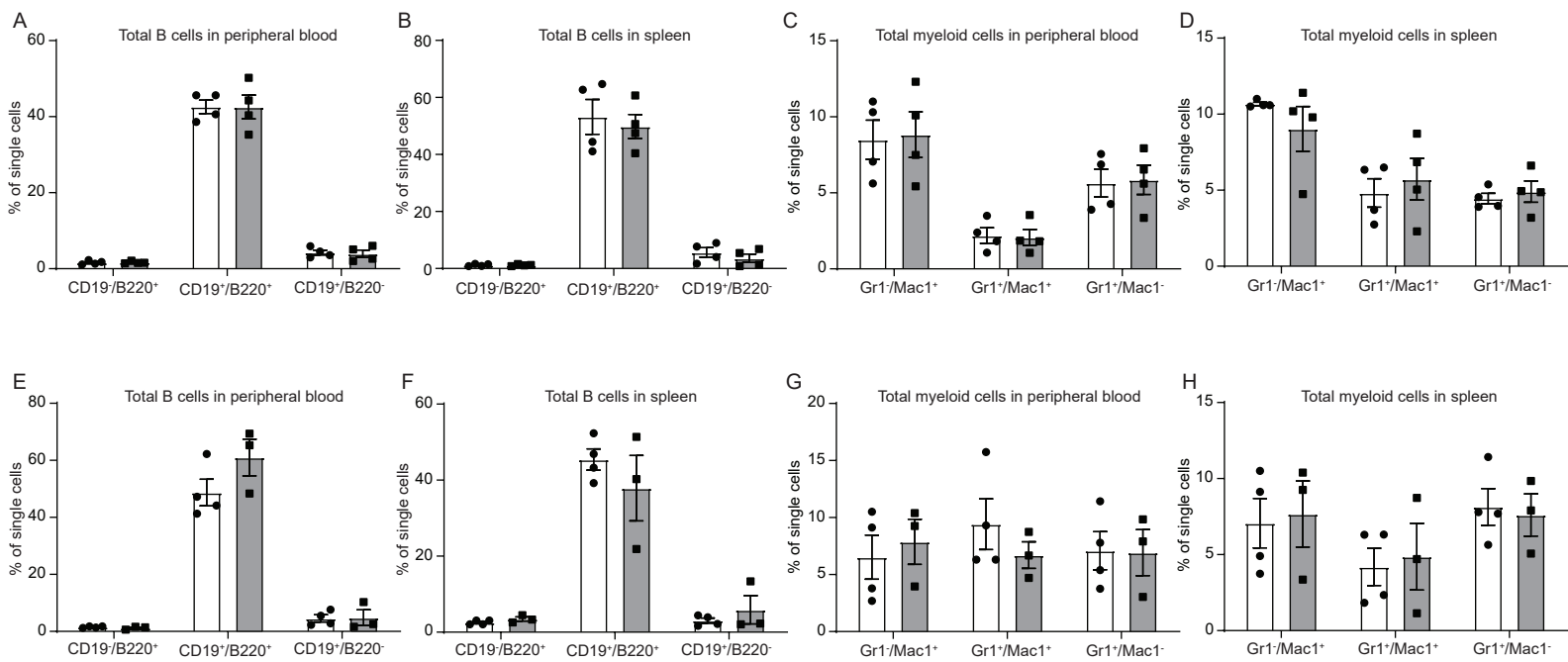
Supplementary Figure 9. Generation of *Arid5b* knock-out mouse models. Schematic diagram of *Vav1* or *Mb1*-driven *Arid5b* knock-out mouse models.

Figure S10



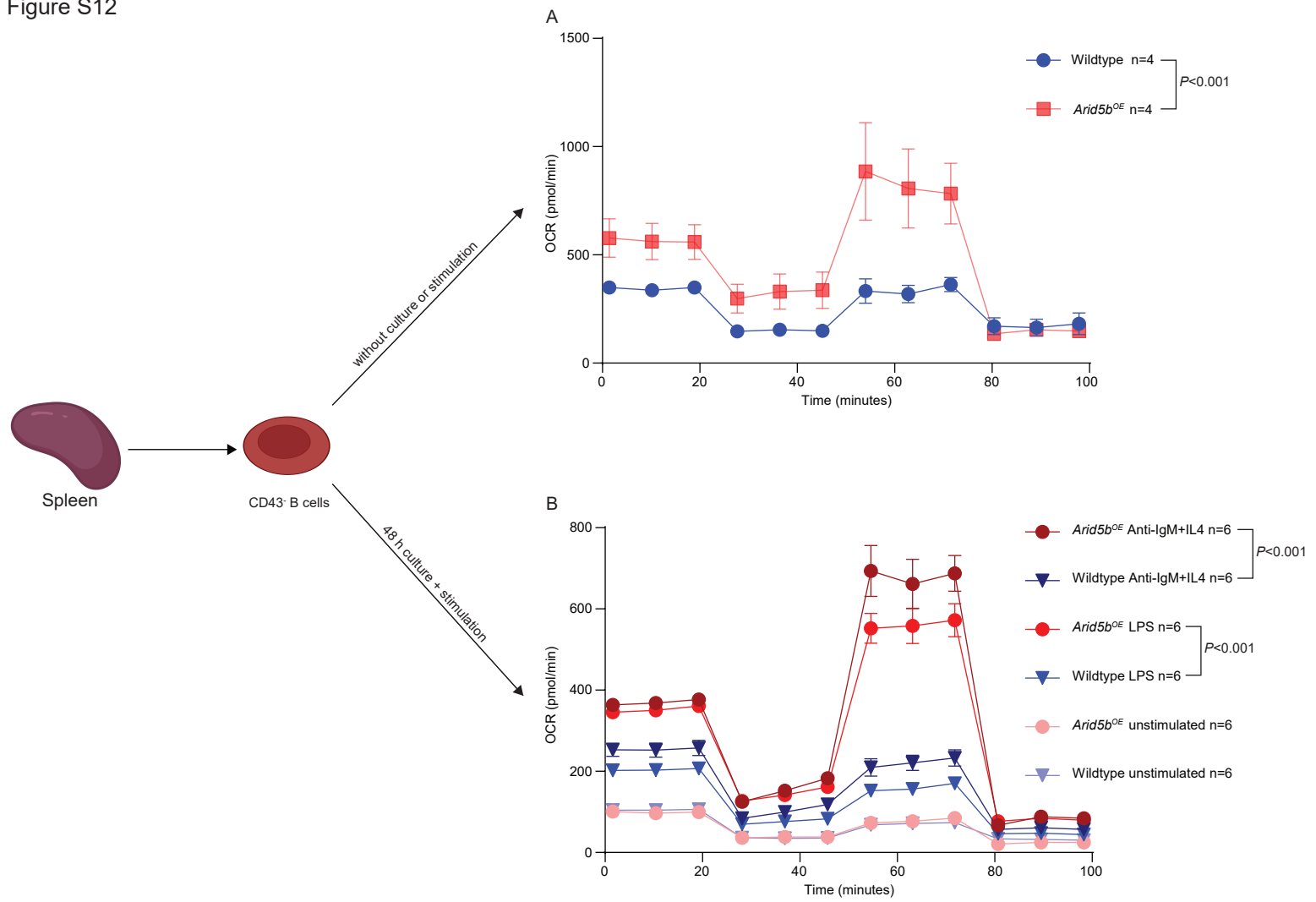
Supplementary Figure 10. Hematopoietic phenotype of bone marrow cells from *Mb1*- and *Vav1*- driven *Arid5b*^{KO} mice. (A-C) Percentage of B-cell subsets (Hardy fractions), hematopoietic stem cells (HSC^{LT} and HSCST) and multi-potent progenitors (MPP2, MPP3, and MPP4), and total Gr1⁺ and Mac1⁺ myeloid cells in the bone marrow of *Mb1*-driven *Arid5b*^{KO} mice (solid bars, n>6) were compared to that of wildtype littermates (open bars, n>5). (D-F) Percentage of B-cell subsets (Hardy fractions), hematopoietic stem cells (HSC^{LT} and HSCST) and multi-potent progenitors (MPP2, MPP3, and MPP4), and total Gr1⁺ and Mac1⁺ myeloid cells in the bone marrow of *Vav1*-driven *Arid5b*^{KO} mice (solid bars, n=3) were compared to that of wildtype littermates (open bars, n=4). *P* value was estimated by two-tail *t* test. *: *P*<0.05; **: *P*<0.01.

Figure S11



Supplementary Figure 11. Hematopoietic phenotypes of peripheral blood and spleen cells from *Mb1*- and *Vav1*-driven *Arid5b*^{KO} mice. (A-B) Total B220⁺ and CD19⁺ B cells in the peripheral blood and spleen of *Mb1-Arid5b*^{KO} mice (solid bars, n=4) compared to wildtype littermates (open bars, n=4). (C-D) Total Gr1⁺ and Mac1⁺ myeloid cells in the peripheral blood and spleen of *Mb1-Arid5b*^{KO} mice (solid bars, n=4) compared to wildtype littermates (open bars, n=4). (E-F) Total B220⁺ and CD19⁺ B cells in the peripheral blood and spleen of *Vav1-Arid5b*^{KO} mice (solid bars, n=3) compared to wildtype littermates (open bars, n=4). (G-H) Total Gr1⁺ and Mac1⁺ myeloid cells in the peripheral blood and spleen of *Vav1-Arid5b*^{KO} mice (solid bars, n=3) compared to wildtype littermates (open bars, n=4). *P* value was estimated by two-tail *t* test.

Figure S12



Supplementary Figure 12. Overexpression of *Arid5b* results in increased OXPPOS of B cells. (A) Seahorse extracellular flux analysis measurement of oxygen consumption rate (OCR) in naive B cells. Naive B cells isolated from *Arid5b*^{OE} mice had increased OCR when compared to naive B cells from wildtype littermates ($P < 0.001$). (B) Seahorse extracellular flux analysis measurement of OCR in B cells stimulated by LPS and IgM F(ab')₂ fragment and IL-4. The baseline OCR of *Arid5b*^{OE} stimulated B cells were higher than wildtype and showed greater maximum mitochondrial respiration capacity, after stimulation with either LPS or IgM F(ab')₂ fragment and IL-4 ($P < 0.001$). P values were estimated using two-way ANOVA.